Supplementary Information

Minimizing ion/electron pathways through ultrathin conformal holey graphene encapsulation in Li- and Mn-rich layered oxide cathodes for high-performance lithium-ion batteries

Sungwook Kim,[a] Jeonguk Hwang,[b] Youngseok Jo,[a] Changyong Park, [b] Neetu Bansal,[c] Rahul R. Salunkhe,[c] Heejoon Ahn *[a, b, d, e]*

[a]Department of Battery Engineering, Hanyang University, 222 Wangsimni-ro, Seongdong-gu, Seoul, 04763, Republic of Korea

[b]Department of Organic and Nano Engineering, Hanyang University, 222 Wangsimni-ro, Seongdong-gu, Seoul, 04763, Republic of Korea

[c]Materials Research Laboratory, Department of Physics, Indian Institute of Technology, NH-44, Jammu 181221, Jammu and Kashmir, India

[d]Human-Tech Convergence Program, Department of Organic and Nano Engineering, Hanyang University, 222 Wangsimni-ro, Seongdong-gu, Seoul, 04763, Republic of Korea

[e]Institute of Nano Science and Technology, Hanyang University, 222 Wangsimni-ro, Seongdong-gu, Seoul 04763, Republic of Korea

*Corresponding authors: E-mail: ahn@hanyang.ac.kr (Heejoon Ahn),
rahul.salunkhe@iitjammu.ac.in (Rahul R. Salunkhe)*

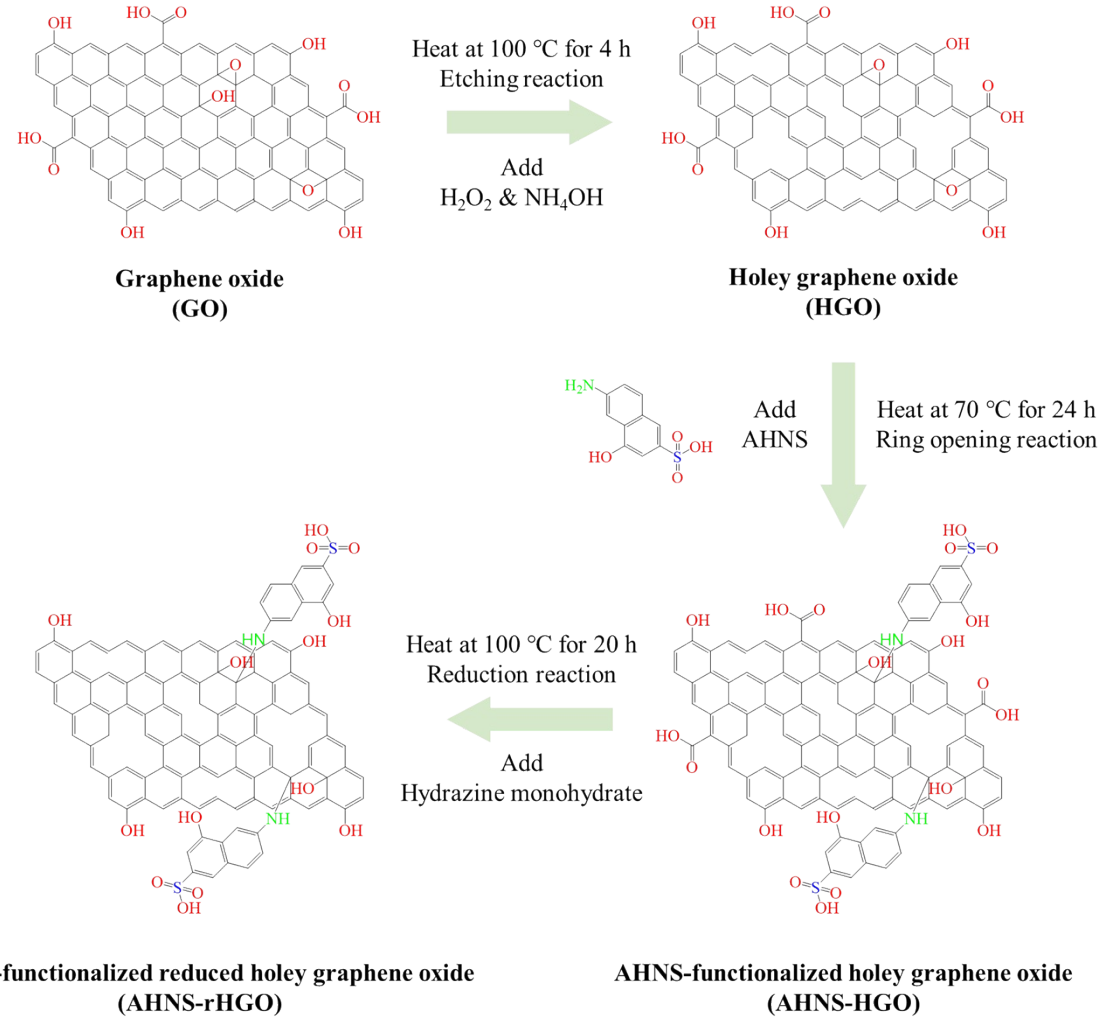

Fig. S1 Schematic for the synthesis of AHNS-rHGO.

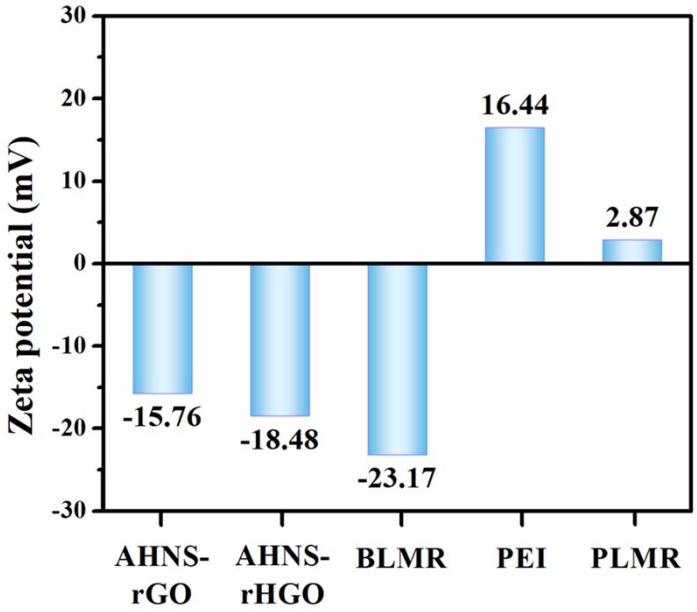

Fig. S2 Zeta potentials of the samples used in the coating process.

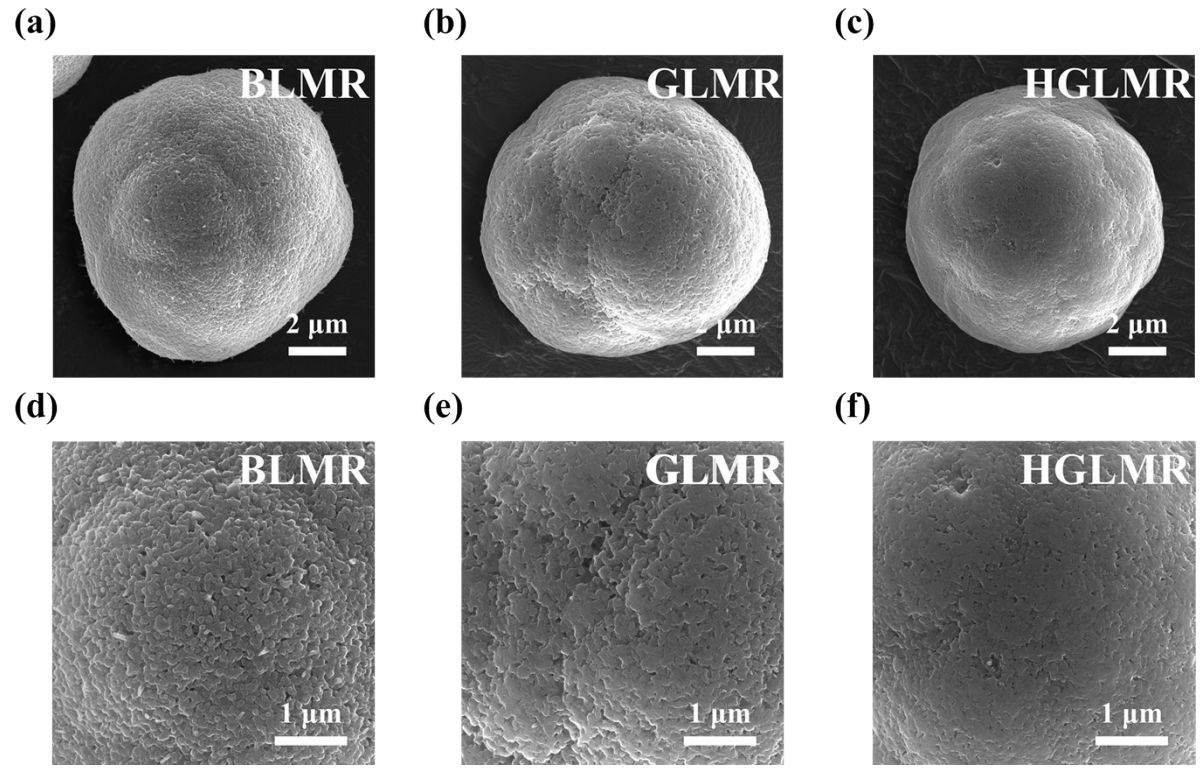

Fig. S3 FE-SEM images of (a, d) BLMR, (b, e) GLMR, and (c, f) HGLMR taken at different magnifications.

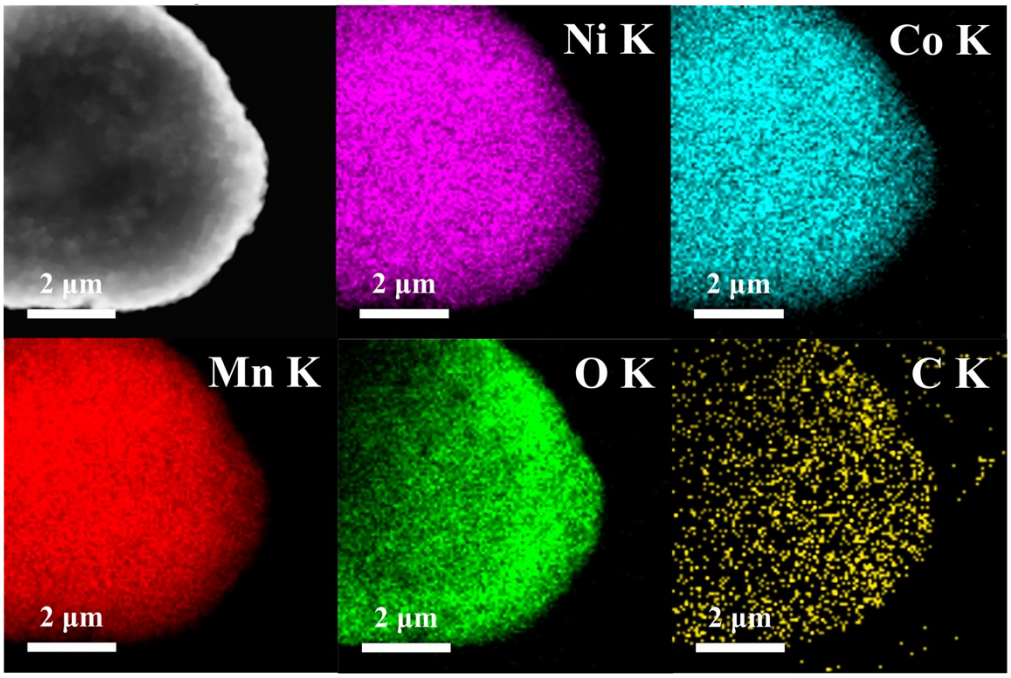

Fig. S4 TEM-EDS mapping images of HGLMR.

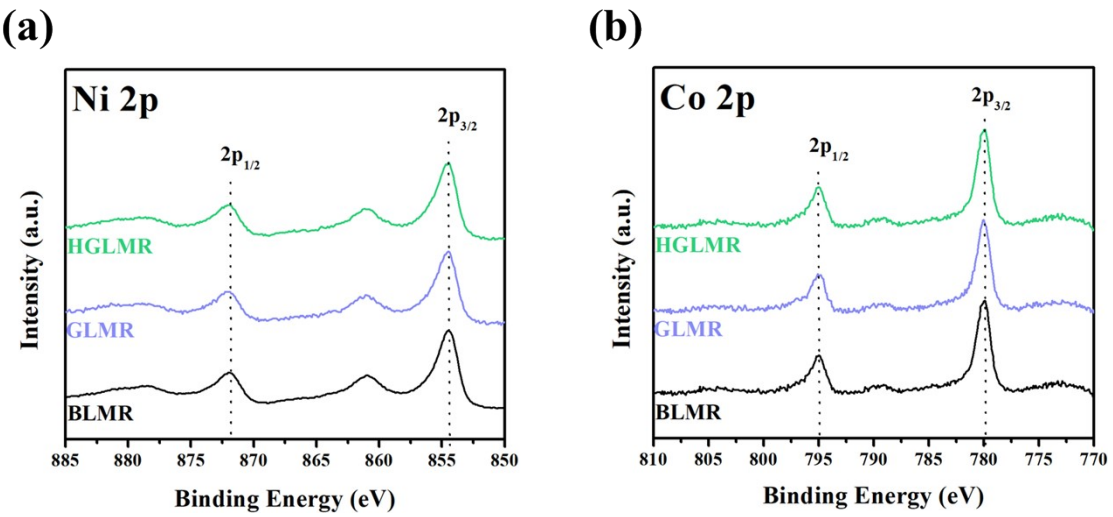

Fig. S5 (a) Ni 2p and (b) Co 2p XPS spectra of BLMR, GLMR, and HGLMR.

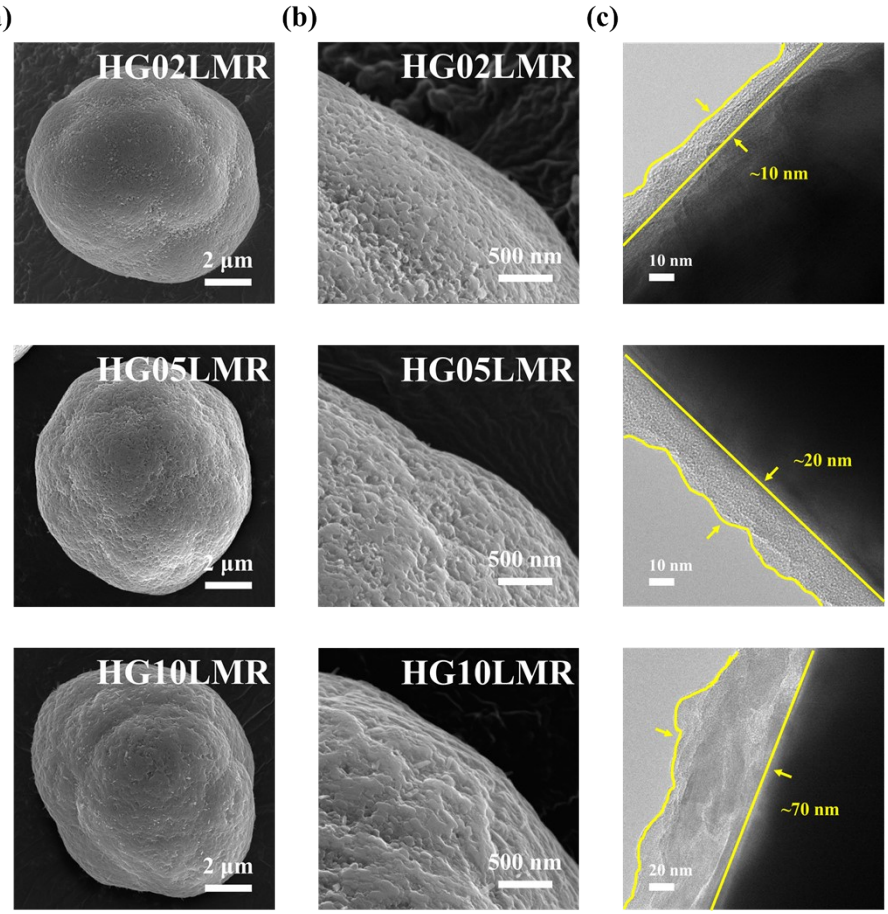

Fig. S6 (a–c) FE-SEM and HR-TEM images of HG02LMR, HG05LMR, and HG10LMR.

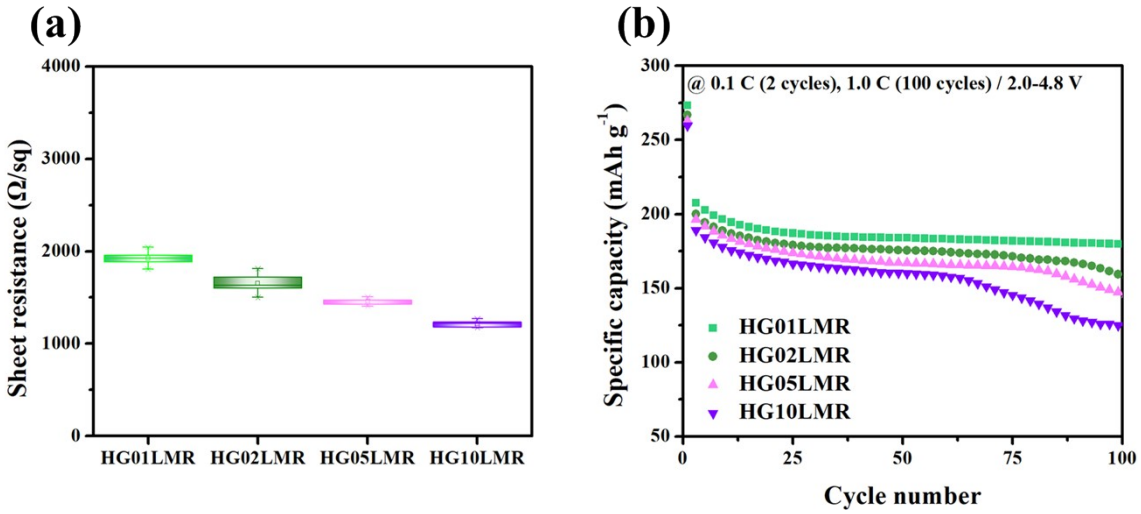

Fig. S7 (a) Sheet resistance values of the electrodes based on carbon contents. (b) Cycling performance based on carbon contents at 1.0 C.

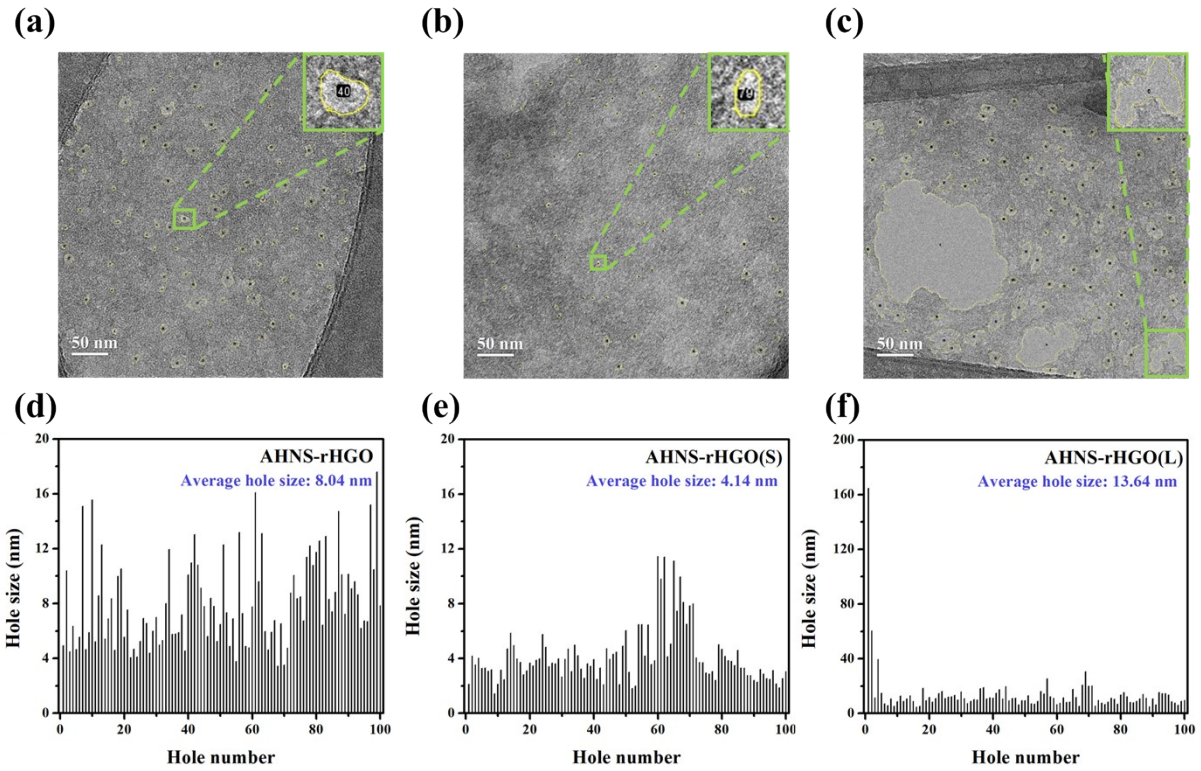

Fig. S8 (a–c) HR-TEM images of AHNS-rHGO, AHNS-rHGO(S), and AHNS-rHGO(L). (d–f) Histograms of the pore size distribution for 100 pores in each HR-TEM image given above.

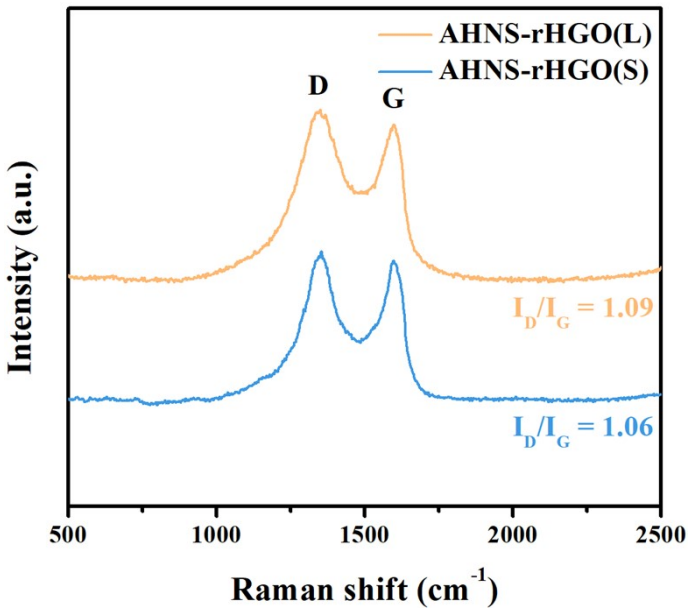

Fig. S9 Raman spectra of AHNS-rHGO(S) and AHNS-rHGO(L).

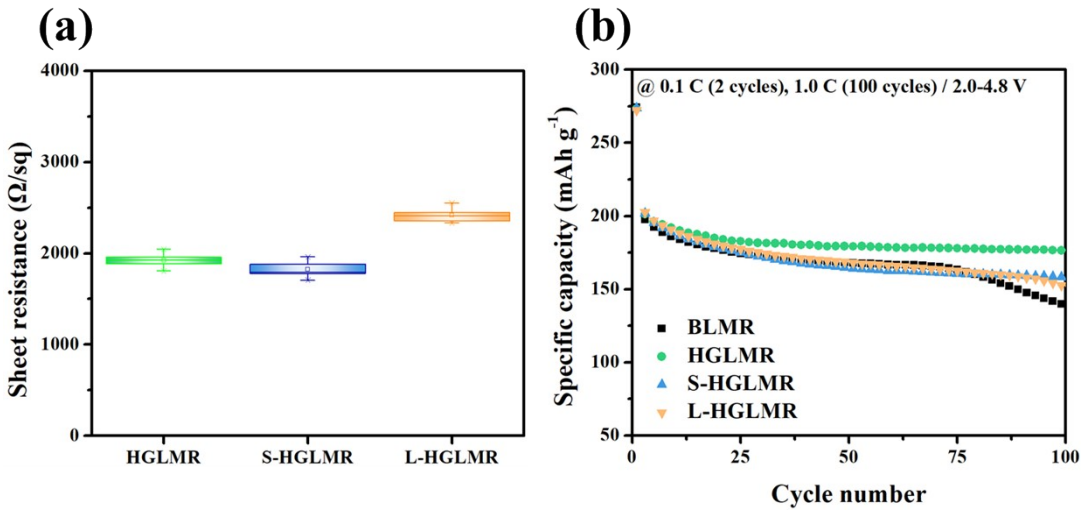

137

138 **Fig. S10** (a) Sheet resistances of the HGLMR, S-HGLMR, and L-HGLMR electrodes. (b) cycling
139 performance of the BLMR, HGLMR, S-HGLMR, and L-HGLMR electrodes.

140

141

142

143

144

145

146

147

148

149

150

151

152

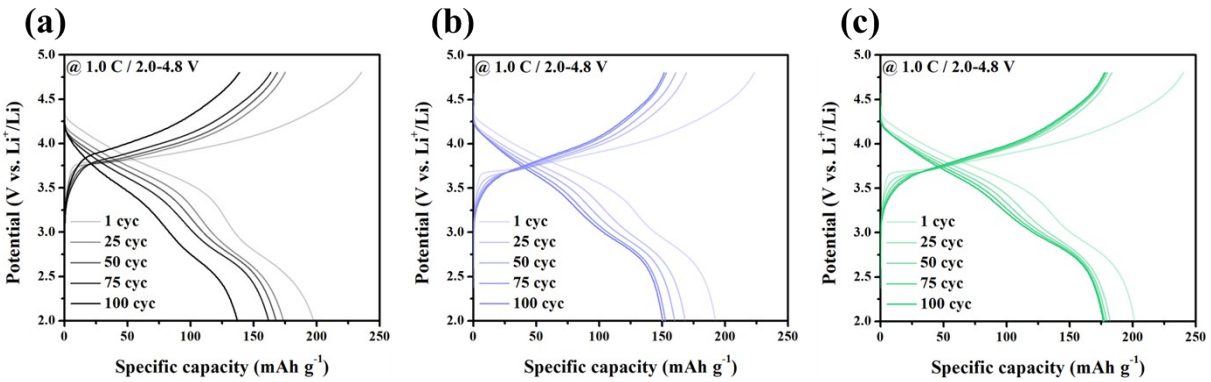

Fig. S11 (a–c) GCD curves illustrating the specific capacities of BLMR, GLMR, and HGLMR for each cycle.

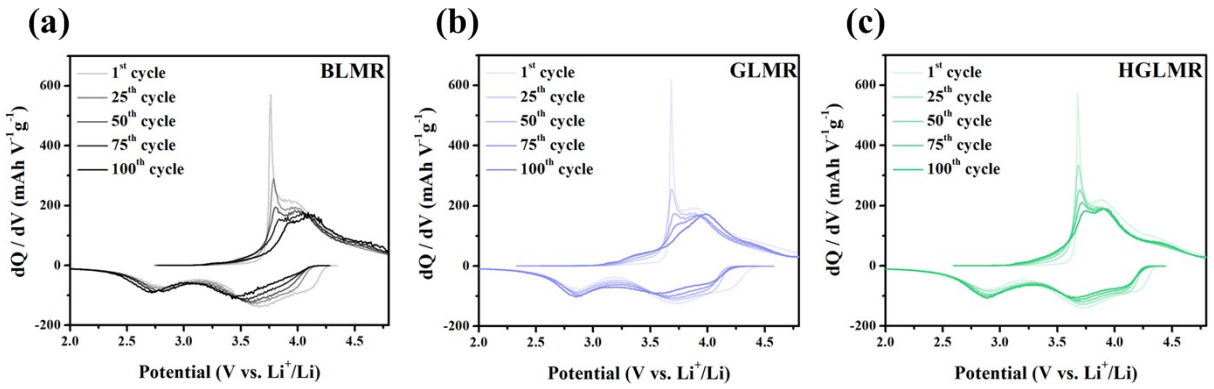

Fig. S12 (a–c) dQ/dV curves for BLMR, GLMR, and HGLMR for each cycle.

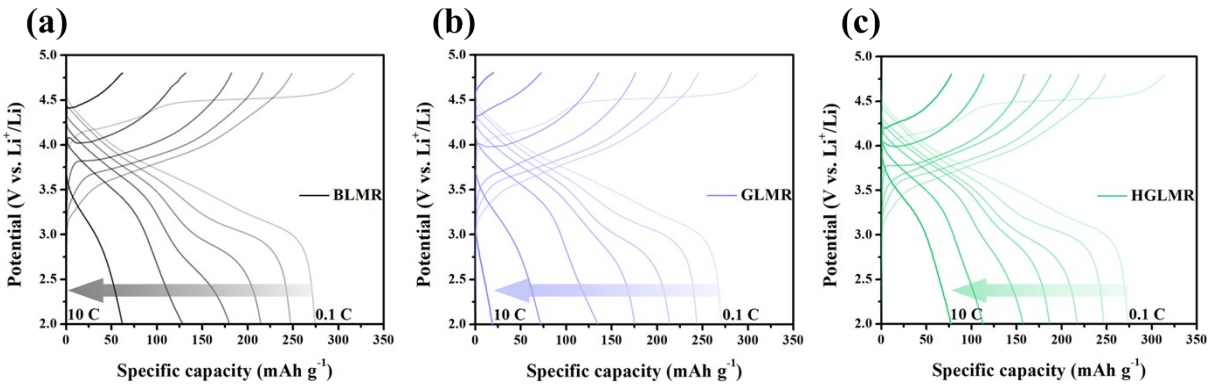

Fig. S13 (a–c) GCD curves of the BLMR, GLMR, and HGLMR electrodes at various C-rates.

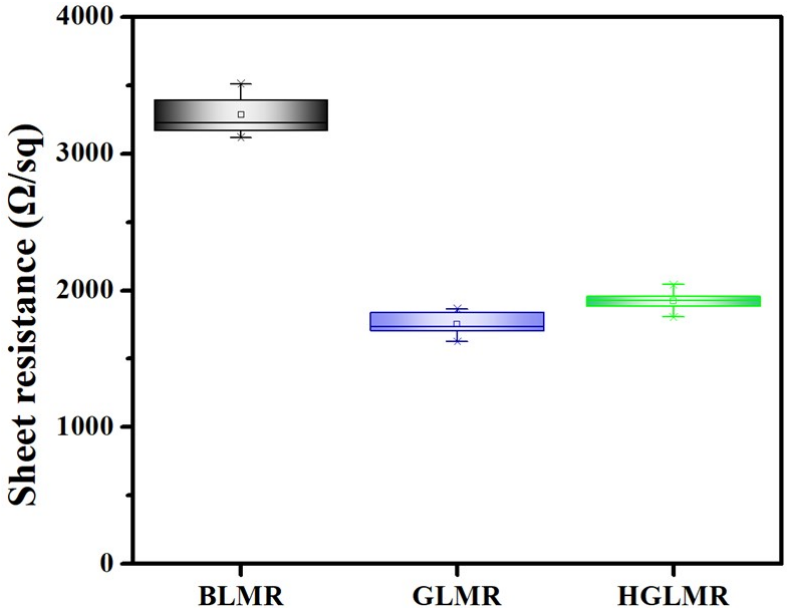

Fig. S14 Sheet resistance values of the BLMR, GLMR, and HGLMR electrodes.

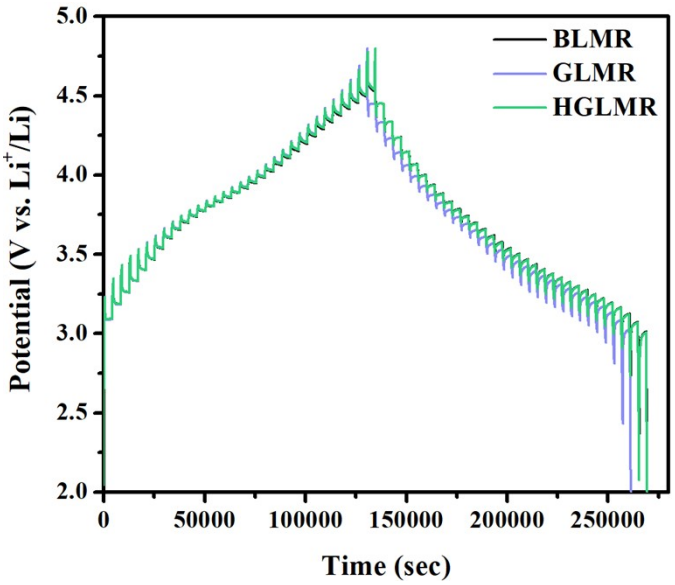

218 .

219 **Fig. S15** GITT curves of the BLMR, GLMR, and HGLMR electrodes.

220

221

222

223

224

225

226

227

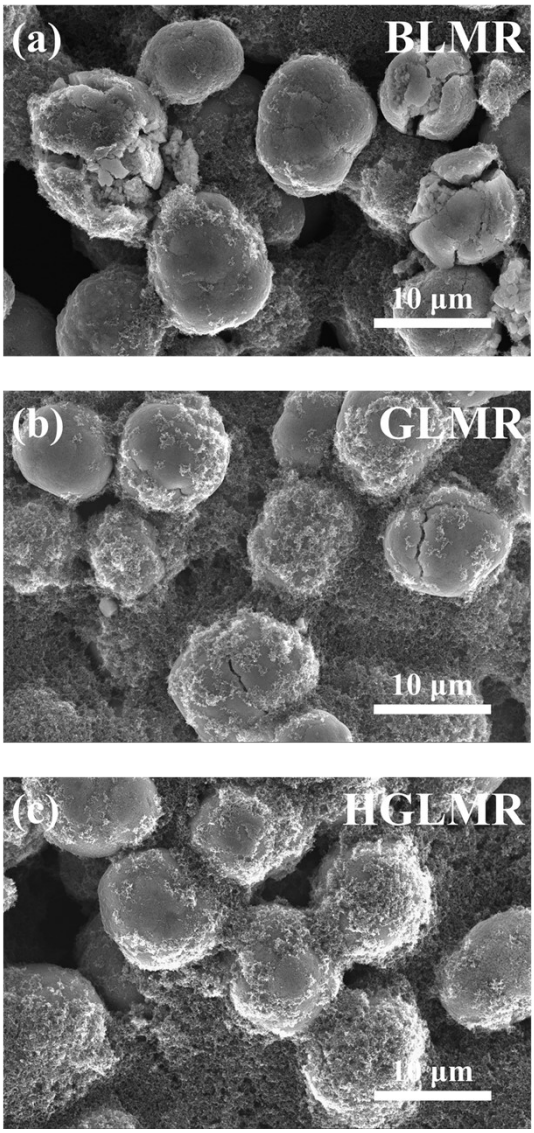

228

229 **Fig. S16** Top-view FE-SEM images of the BLMR, GLMR, and HGLMR electrodes after 100 cycles.

230

231

232

Table S1 ICP-OES analysis of the BLMR, GLMR, and HGLMR particles.

Sample	Analysis results (weight %)			
	Li	**Ni**	**Co**	**Mn**
BLMR	10.05	12.57	6.33	40.07
GLMR	10.04	12.24	6.16	39.06
HGLMR	9.97	12.05	6.06	38.83

Table S2 BET analysis of the BLMR, GLMR, and HGLMR electrodes.

Sample	Specific surface area ($m^2\ g^{-1}$)	Total pore volume ($cm^3\ g^{-1}$)	Average pore size (nm)
BLMR	3.947	0.005239	34.137
GLMR	4.2701	0.006089	37.649
HGLMR	4.3092	0.006232	38.679

Table S3 Tap density analysis results for BLMR, GLMR, and HGLMR.

Sample	Tap density (g cm^{-3})
BLMR	2.859
GLMR	2.808
HGLMR	2.804

Table S4 Areal ratio variation in the XPS depth profiles of F 1s based on etching times from 0 to 100 s.

Composition (%)	BLMR			GLMR			HGLMR		
	Etching time (s)								
	0	50	100	0	50	100	0	50	100
LiF	41.3	63.4	65.6	11.3	44.0	49.5	9.8	33.9	40.6
$Li_xPO_yF_z$	19.1	15.6	17.2	-	1.4	14.8	-	3.8	17.6
CF_2	39.6	20.8	17.2	88.7	54.6	35.7	90.2	62.3	41.8

Table S5 Comparison of electrochemical performances of the HGLMR electrode with previously reported surface-coated LMR electrodes.

Cathode material	Coating material	Mass loading (mg cm^{-2})	Voltage window (V)	Rate capability	Cycle stability	Ref
$Li_{1.2}Ni_{0.13}Co_{0.13}Mn_{0.54}O_2$	$LiErO_2$	2.0–3.0	2.0–4.7	162.1 mAh g^{-1} at 5.0 C	80% after 100 cycles at 1.0 C	[1]
$Li_{1.2}Ni_{0.13}Co_{0.13}Mn_{0.54}O_2$	Li_2ZrO_3	3	2.0–4.8	155.6 mAh g^{-1} at 5.0 C	89% after 150 cycles at 1.0 C	[2]
$Li_{1.2}Ni_{0.13}Co_{0.13}Mn_{0.54}O_2$	$KMnO_4$	2.0	2.0–4.8	91.6 mAh g^{-1} at 10.0 C	88% after 170 cycles at 0.2 C	[3]
$Li_{1.2}Ni_{0.13}Co_{0.13}Mn_{0.54}O_2$	$(NH_4)_2SiF_6$	2.0	2.0–4.8	76.0 mAh g^{-1} at 10.0 C	90.4% after 100 cycles at 1.0 C	[4]
$Li_{1.2}Ni_{0.13}Co_{0.13}Mn_{0.54}O_2$	In_2O_3	1.3	2.0–4.8	109.1 mAh g^{-1} at 5.0 C	80% after 200 cycles at 1.0 C	[5]
$Li_{1.2}Ni_{0.13}Co_{0.13}Mn_{0.54}O_2$	PO_4^{3-}-doped layer@spinel @rGO	1.35	2.0–4.8	82.3 mAh g^{-1} at 10.0 C	86.5% after 200 cycles at 1.0 C	[6]
$Li_{1.2}Ni_{0.13}Co_{0.13}Mn_{0.54}O_2$	Graphene quantum dot	1.2	2.0–4.8	113.2 mAh g^{-1} at 5.0 C	86.5% after 150 cycles at 1.0 C	[7]
$Li_{1.2}Ni_{0.2}Mn_{0.6}O_2$	N-doped Graphene	3.5	2.0–4.8	≈ 100.0 mAh g^{-1} at 8.0 C	86% after 200 cycles at 0.2 C	[8]
$Li_{1.2}Ni_{0.13}Co_{0.13}Mn_{0.54}O_2$	$Li_{1.4}Y_{0.4}Ti_{1.6}PO_4$	2.65	2.0–4.8	78.3 mAh g^{-1} at 10.0 C	83.2% after 100 cycles at 1.0 C	[9]
$Li_{1.2}Ni_{0.16}Co_{0.08}Mn_{0.56}O_2$	**PEI/reduced holey graphene oxide**	**4**	**2.0–4.8**	**78.0 mAh g^{-1} at 10.0 C**	**87.8% after 100 cycles at 1.0 C**	**This work**

References

1. Z. Wei, D. Zhang, J. Zhong, C. Zheng, J. Feng, and J. Li, *Batteries Supercaps*, 2023, **6**, e202200568.
2. J. Chen, S. Cao, Z. Li, H. Li, C. Guo, R. Wang, L. Wu, Y. Zhang, Y. Bai, and X. Wang, *ACS Appl. Mater. Interfaces*, 2023, **15**, 36394–36403.
3. T. Wei, X. Qin, C. Lei, and Y. Zhang, *J. Alloy. Compd.*, 2022, **895**, 162647.
4. Q. Luo, J. Kang, Z. Liao, X. Feng, H. Zou, W. Yang, C. Pai, R. Waiyin Sun, and S. Chen, *ACS Appl. Energy Mater.*, 2022, **5**, 4641–4650.
5. M. Yu, X. Wei, X. Min, A. Yuan, and J. Xu, *Mater. Chem. Phys.*, 2022, **286**, 126228.
6. M. Zhao, Y. Wang, Y. Wang, S. Liu, Z. Chen, F. Yong, P. Qian, S. Yang, Q. Huang, and Z. Ning, *J. Alloy. Compd.*, 2024, **983**, 173822.
7. M. Yu, X. Wei, X. Min, A. Yuan, and J. Xu, *Energy Fuels*, 2022, **36**, 5502–5512.
8. M. Chen, G. Zhang, B. Wu, M. Liu, J. Chen, W. Xiang, and W. Li, *ACS Appl. Energy Mater.*, 2022, **5**, 4307–4317.
9. A. Li, C. Qian, G. Mao, Z. Liu, Z. Li, Y. Zhang, L. Yin, L. Shen, and H. Li, *J. Power Sources*, 2024, **599**, 234245.